Depletion of the RNA binding protein QKI and circular RNA dysregulation in T-cell acute lymphoblastic leukemia

This study investigates the impact of abnormally low QKI expression on the T-cell acute lymphoblastic leukemia (T-ALL) circRNAome.

Circular RNA (circRNA) drive oncogenic processes, acting as both oncogenic and tumor suppressor molecules.[1] Recent data on aberrant circRNA expression and functional impact in T-ALL[2] incited further study of the factors underlying circRNA dysregulation in this malignancy. An interesting lead to pursue was the observation that the splicing factor Quaking (QKI), previously linked to circRNA biogenesis,[3,4] might be dysregulated in T-ALL. QKI is considered a tumor suppressor protein[5] and has reduced expression in solid cancer.[6] Less is known about it in leukemias. Heterogeneous *QKI* expression has been shown in B-cell ALL, with *QKI* downregulation in pediatric subtypes of leukemia.[7] MiR-155-dependent-QKI depletion has been implicated in inflammation in chronic lymphocytic leukemia.[8] In T-ALL, *QKI* downregulation was reported in cases with high *HOXA* expression, carrying *CALM-AF10*[9] or *KMT2A* rearrangements.[10] The *QKI* transcript displayed a highly heterogeneous level of expression in T-ALL (range, 0-15 transcripts per million) (Figure 1A), according to RNA-sequencing data in 25 pediatric patients[11] representing five T-ALL molecular subtypes.[2] Two groups of patients with normal (QKI_normal) and aberrantly low (QKI_low) *QKI* expression (Figure 1A) were defined by comparison with their normal counterparts, five thymocyte populations from two healthy donors including three $CD34^+$ early maturation and two $CD4^+CD8^+$ stages of the $\alpha\beta$ lineage.[2] CircComPara2[12] identified 3,376 circRNA expressed in the T-ALL samples, with an average of five circular isoforms per gene, and 20 genes with at least 15 circular isoforms, including *TASP1* and *CASC15*, each with 30 circRNA. A major effect of the T-ALL molecular subtypes on circRNA expression is known.[2,9] Since *QKI* expression is not independent of T-ALL molecular subtypes in this cohort (significant association between the *QKI* expression group and subtypes $P<0.01$), all statistical analyses of circRNA profiles in relation to *QKI* expression were conducted using the molecular subtypes as covariates to bring to light the net effect of *QKI* variation on circRNA expression level in T-ALL.

Unsupervised analysis of circRNA expression profiles showed that patients' samples separate in a gradient coincident with increasing *QKI* levels (Figure 1B). The separation was less clear with the linear counterpart of circRNA-expressing genes and the circRNA expression variation in QKI_low *vs.* QKI_normal T-ALL was more marked than the variation of the linear counterpart (*Online Supplementary Figure S1A, B*). We identified 209 circRNA with expression significantly correlated with *QKI* level (Spearman coefficient, $|rho|>0.4$, adjusted Benjamini-Hochberg, $P<0.05$), 96 with positive and 113 with negative correlation (Figure 1C), as exemplified by circUBAP2 and circMAN1A2, with a profile strongly directly and inversely correlated with *QKI* expression and high abundance.

Next, we examined the differences in circRNA expression among the groups of patients in relation to *QKI* level using multiple approaches, including machine learning techniques (DaMiRseq R package). Random forest analysis identified a subset of 149 circRNA that classify T-ALL cases with low and normal *QKI* expression (Figure 1D). The importance of each circRNA in the classification model was prioritized using accuracy loss upon circRNA exclusion and circRNA contribution to the homogeneity of the nodes and leaves in the resulting random forest (Gini score) (*Online Supplementary Figure S1C*).

Regulatory activity at the splicing level is expected to result in a variation in both the absolute circRNA expression and the relative circRNA expression compared to the linear counterpart (circular to linear proportion, CLP). A varied absolute circRNA expression level, with a stable CLP across conditions, indicates that the change in circRNA expression across conditions follows the linear expression pattern, likely being controlled at the transcriptional level. Instead, a CLP variation across conditions highlights an uncoupling of circRNA and linear expression variation.

The comparison of QKI_low with QKI_normal T-ALL circRNAomes identified 328 and 425 circRNA with significantly varied (edgeR; robust estimation of dispersion; adjusted Benjamini-Hochberg, $P<0.1$) expression (DE) and CLP (DP; CircTest[2]), respectively (Figure 1E). Considering absolute and relative circRNA expression, equal numbers of circRNA were over- or less expressed in the QKI_low group (Figure 1F, *Online Supplementary Table S1*). CircPHACTR4 was downregulated in association with reduced *QKI* expression. For 133 and 37 circRNA, a concordant significant increase and decrease, respectively, in both expression level and CLP was recorded when comparing QKI_low with QKI_normal cases. CircRNA with increased CLP and stable expression, such as circRNA derived from *SCRG1* and *FLG-AS1* genes (*Online Supplementary Table S1*), indicated that QKI reduction may shift the equilibrium of circular and linear splicing in T-ALL. Importantly, 165 (28%) of the circRNA with absolute or relative expression changes in the QKI_low group had been previously found to be dysregulated in this malignancy,[2] indicating that abnormally low QKI expression can explain, at least in part, circRNA dysregulation in T-ALL.

CircRNA modulated by the QKI level, highly expressed in

T-ALL and dysregulated, in comparison with their normal counterparts, are shown in Figure 1G. CircRNA upregulated linked to low QKI expression that were previously associated with oncogenic functions in other malignancies include circRTN4[13] and circTDRD3.[14] Overall, T-ALL patients stratified by QKI expression levels have different circRNAomes, with an abnormally reduced QKI level associated with a significant variation in absolute circRNA expression and a more marked change in the CLP.

Further data were obtained using QKI expression manipulation in T-ALL *in vitro*, choosing Jurkat cells with high endogenous QKI expression. About $4x10^6$ cells were transfected with 20 nM of NTC or QKI siRNA (ON-TARGETplus SMARTpool siRNA; Dharmacon®) using the Neon transfection system (Thermo Fisher). RNA was extracted 72 hours after transfection using a QIAGEN RNeasy Plus mini kit and assessed for integrity. Efficiently silenced *QKI* (QKI_KD) (Figure 2A) and control (CTR) RNA-sequencing profiling (Illumina Truseq stranded total RNA) showed that the global circRNA expression profile was affected by *QKI* KD in T-ALL cells *in vitro* (Figure 2B). CircSUCO and circDNMT3B were among the most upregulated circRNA upon *QKI* silencing, whereas circPHACTR4 and circKLHDC1 showed dramatic reductions. Previous studies have shown that QKI favors the biogenesis of certain circRNA.[3] However, equal numbers of circRNA with an absolute expression increase (47.8%) and decrease (52.2%) upon *QKI* KD in T-ALL *in vitro* were observed. Figures were similar considering only the 50% most abundant circRNA and circRNA with an absolute log fold change higher than two (Figure 2C). These results are in line with a recent report that *QKI* knockout sustains the expression of certain circRNA while suppressing others in mice cardiomyocytes.

Importantly, as we observed in patients, *QKI* silencing in

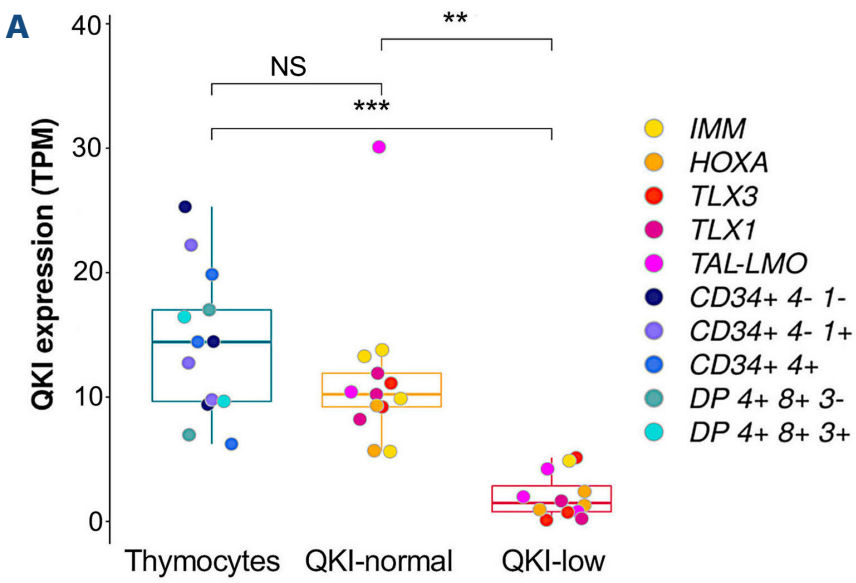

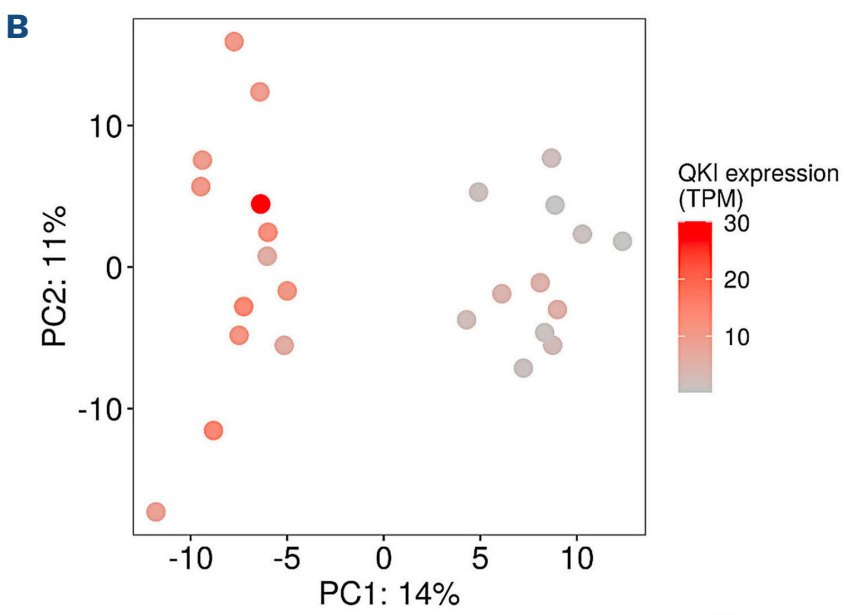

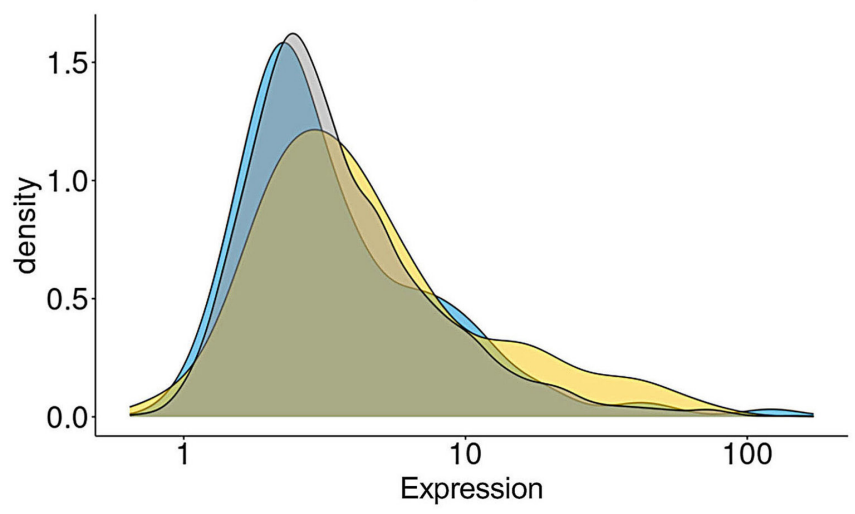

circ/QKI correlation	N	mean	SD
negative	113	5.9	12.6
positive	96	7.7	11.1
none	3167	5.3	8.9

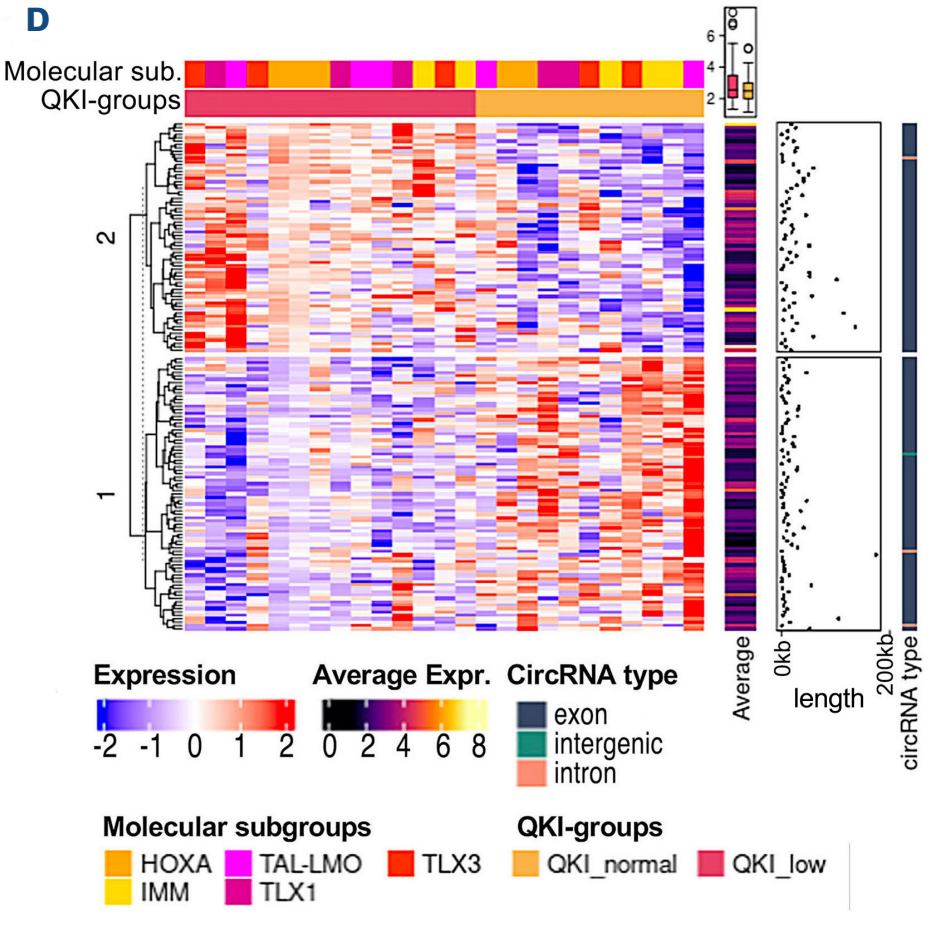

Continued on following page.

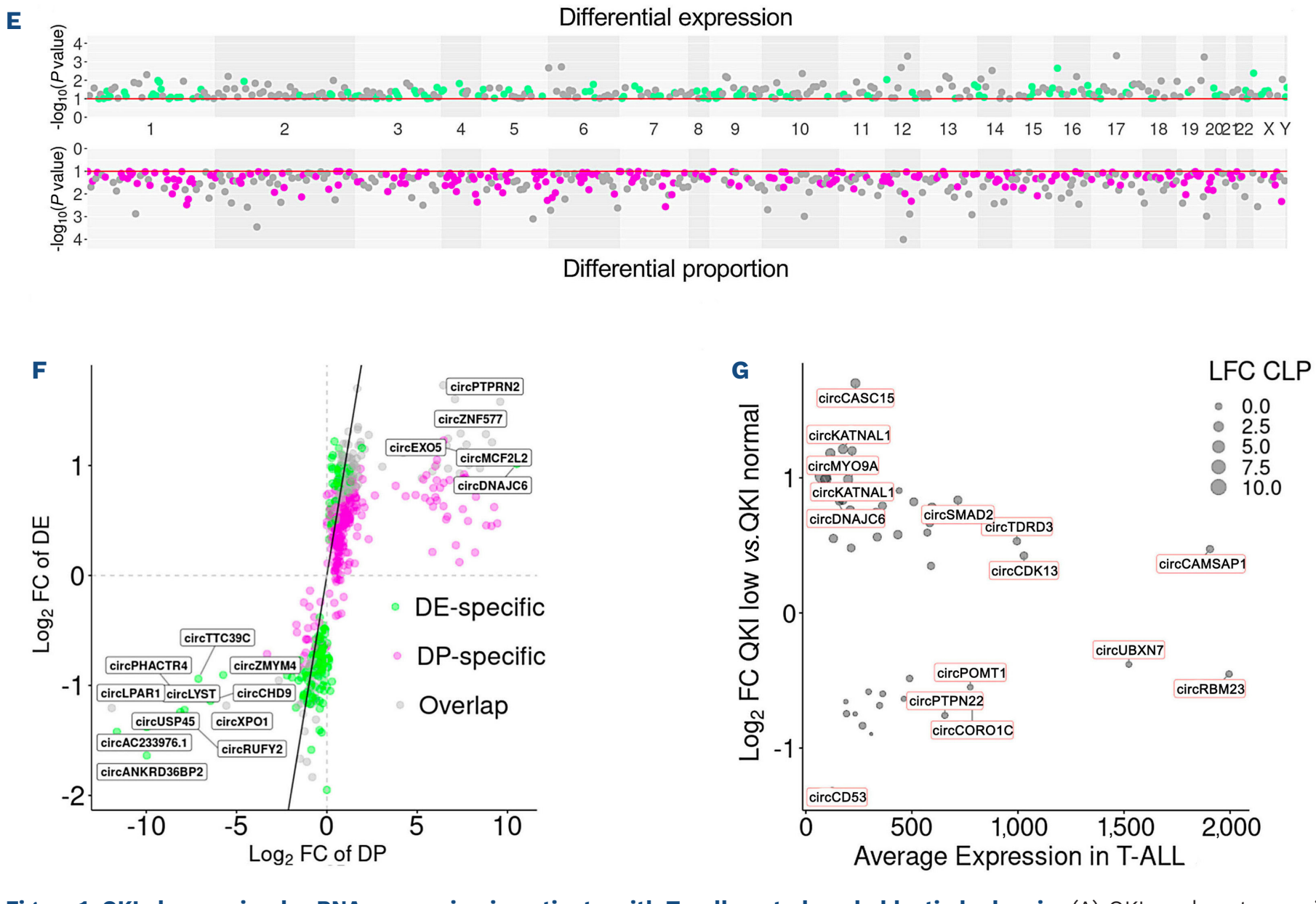

Figure 1. QKI shapes circular RNA expression in patients with T-cell acute lymphoblastic leukemia. (A) QKI nuclear transcript normalized expression in normal developing thymocytes allowed the definition of two groups (QKI_low, QKI_normal) of T-cell acute lymphoblastic leukemia (T-ALL) (**P≤0.01; ***P≤0.001; NS: not statistically significant; Mann-Whitney test). (B) Unsupervised principal component analysis of circular RNA (circRNA) expression profiles separated T-ALL patients (N=25) according to a gradient of *QKI* expression levels. (C) Expression distribution of circRNA negatively, positively or not correlated with *QKI* expression in T-ALL patients. The table shows the total number, mean, and standard deviation for each subgroup of circRNA defined by its correlation with *QKI* expression. (D) Random forest classification analysis identified circRNA well discriminating QKI_low and QKI_normal T-ALL for which the heatmap shows standardized expression and other characteristics, such as average expression across samples, length of the backsplice and circRNA types. (E) Manhattan plot of *P* values from circRNA with differential expression (DE) and differential proportions (DP). Horizontal red lines indicate a *P* value threshold of 0.1, highlighting the significant DE and DP circRNA. DE-specific and DP-specific circRNA are shown in green and pink, respectively. CircRNA that are shared by DE and DP groups are shown in gray. (F) Scatter plot of log fold-change (FC) of significantly (P≤0.1) DE and DP circRNA comparing QKI_low with QKI_normal T-ALL patients (x- and y-axes show the FC of, respectively, the circular to linear proportion and absolute circRNA expression). DE-specific and DP-specific circRNA are shown in green and pink, respectively. CircRNA that are both DE and DP are shown in gray. (G) Scatterplot of circRNA log FC comparing QKI_low and QKI_normal T-ALL and circRNA average expression in T-ALL; 140 circRNA significantly DE and DP and also among those discriminant between QKI_low *versus* QKI_normal T-ALL are shown; names are shown only for circRNA with an average expression of at least 600 and absolute log FC of at least 1 that were previously reported to be dysregulated in T-ALL by Buratin *et al.*[2] PC: principal component; TPM: transcripts per million; SD: standard deviation; LFC: log fold-change.

T-ALL *in vitro* impacted the CLP, supporting the direct role of this protein in the regulation of backsplicing efficiency. In most cases, the expression variation was associated with a varied CLP (Figure 2D), thus being uncoupled from the variation of the linear counterpart. There was a strong concordance between circRNA expression and proportion variation. The majority (>80%) of circRNA upregulated upon *QKI* KD also had an increased proportion, whereas only about half of the downregulated circRNA also had a reduced CLP (Figure 2D). Isoform-specific regulation of alternative backsplicing was suggested by observation of circRNA isoforms from the same gene with opposite behaviors upon QKI KD (*Online Supplementary Figure S1D*). Moreover, we considered QKI-binding motifs (QKI response elements; QRE) residing in the introns adjacent (1,000 bp) to back splice junctions, according to both cross-linking immunoprecipitation followed by RNA sequencing (CLIP-sequencing) data (CLIPdb and starBase v2.0 databases) and

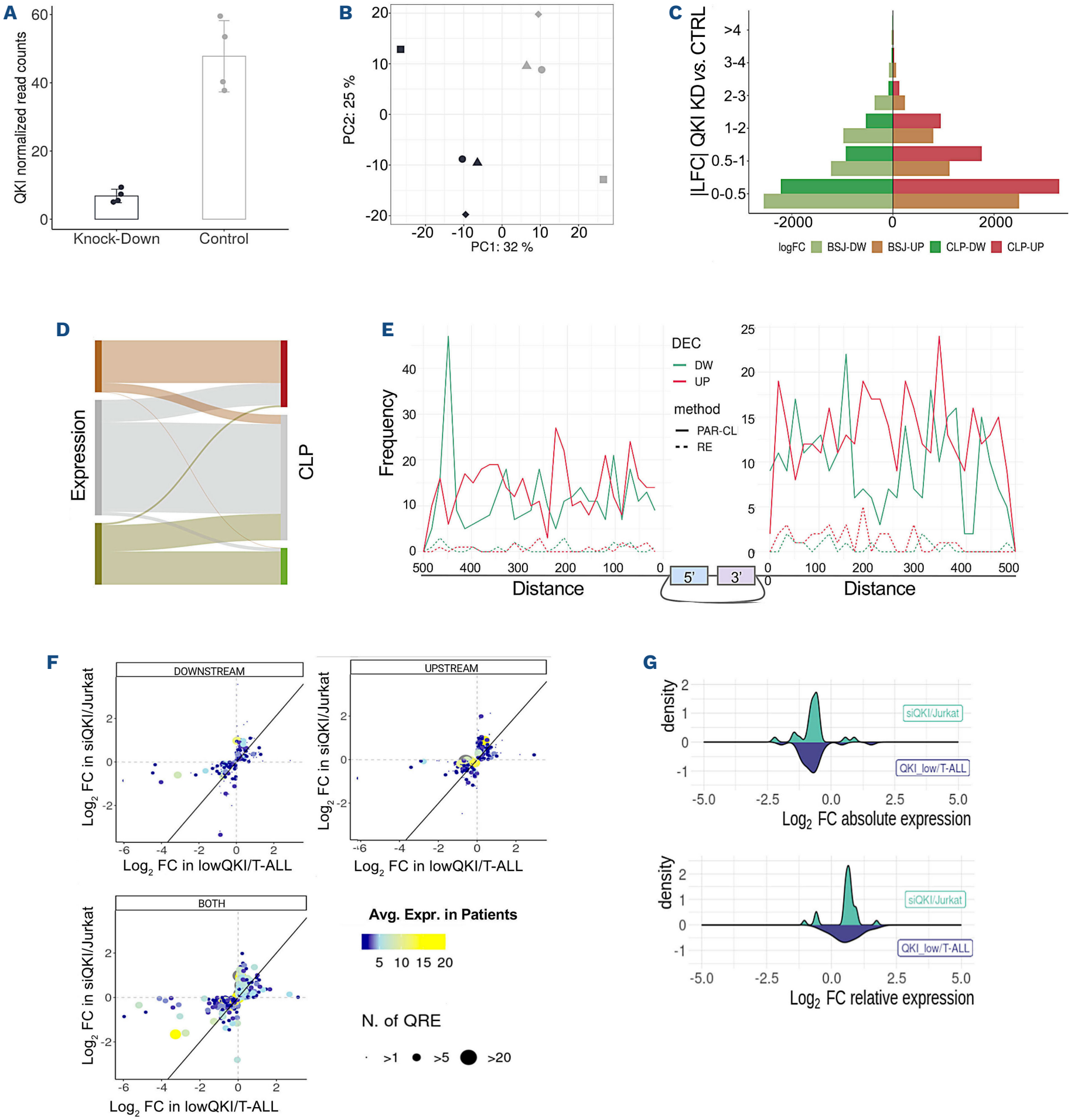

Figure 2. Circular RNA is affected by *QKI* knockdown in T-cell acute lymphoblastic leukemia *in vitro*. (A) *QKI* silencing in Jurkat cells (80% reduction in *QKI* knockdown [QKI_KD] *vs.* control [CTR]). (B) Circular RNA (circRNA) expression separates QKI_KD from CTR samples (principal component analysis based on 10,774 circRNA expression profiles). (C) Barplot of the number of circRNA binned by $\log_2$ fold-change absolute value comparing QKI_KD with CTR. The left and right sides represent the variation in absolute (BSJ) and relative (CLP) expression, respectively. (D) Sankey plot of the intersections of circRNA with expression and/or circular to linear proportion increased, decreased or unvaried upon *QKI* KD. (E) Frequency of QKI response elements (QRE) in the introns flanking the back splice junctions. (F) Scatterplot of log fold-change of circRNA expression variation in QKI_low *versus* QKI_normal T-cell acute lymphoblastic leukemia (T-ALL) patients (x-axis) and upon *QKI* KD in Jurkat cells (y-axis). Data are split according to the position of QRE detection in the flanking introns: only downstream, only upstream, or on both sides. The dots' color reflects the mean relative expression and size of the number of QRE detected in the flanking introns. (G) Mirror density plot of log fold-change of absolute (upper) and relative (bottom) expression variation upon *QKI* silencing in Jurkat cells and in QKI_low *versus* QKI_normal T-ALL patients. PC: principal component; LFC: log fold-change; CLP: circular to linear proportion.

QRE motif predictions (*Online Supplementary Table S2*). QRE were enriched in the upstream flanking regions of downregulated circRNA upon *QKI* KD and in downstream regions of upregulated circRNA (Fisher exact test, *P*=0.049) (Figure 2E). Expression changes, separating circRNA with QRE downstream, upstream or on both sides confirmed this finding, also showing that a higher number of QRE associated with larger expression variation (Figure 2F). Comparing our results in Jurkat cells with those previously observed in HEK293T cells,[3] 540 circRNA exhibited a concordant expression variation (absolute log fold-change at least 0.5) after *QKI* KD in both settings, implying causality. The abundance of circCAMSAP1, circSMARCA5, circPCMTD1 and circMGA with adjacent QKI PAR-CLIP sites was reduced following *QKI* knockdown in both datasets, corroborating our data.

Finally, considering 2,519 circRNA expressed in both patients and Jurkat cells, a good concordance between the model and patients' data emerged: 266 circRNA were evaluable features in model classification and had significant differential expression variation comparing QKI_low *versus* QKI_normal T-ALL cases with a concordant variation of CLP or absolute expression upon *QKI* KD in T-ALL *in vitro* (Figures 2G and 3A). Importantly, in the further comparison of QKI_low T-ALL with thymocytes from healthy donors, most of these circRNA showed significant dysregulation, consistent with the comparison in the groups of patients (Figure 3A).

CircTASP1 (chr20:13528433-13569586, exons 7-10 back-spliced) and circPHACTR4 (chr1:28459085-28466535: exon 2-part of exon 5), which were respectively up- and down-regulated in the QKI-reduced condition in T-ALL, and also had altered expression (8.2 times too high and 7.3 times too low, respectively) in QKI_low T-ALL com-

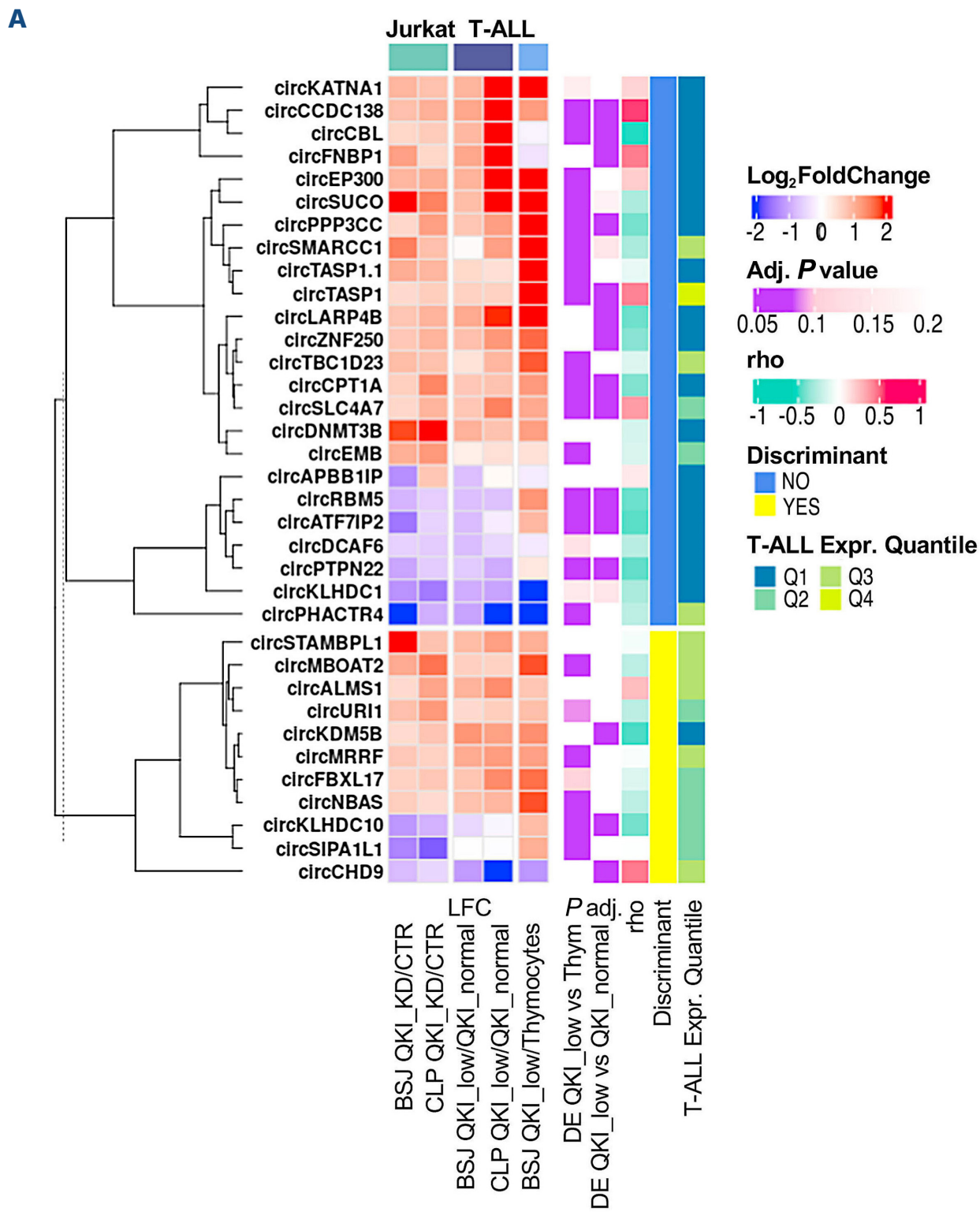

Continued on following page.

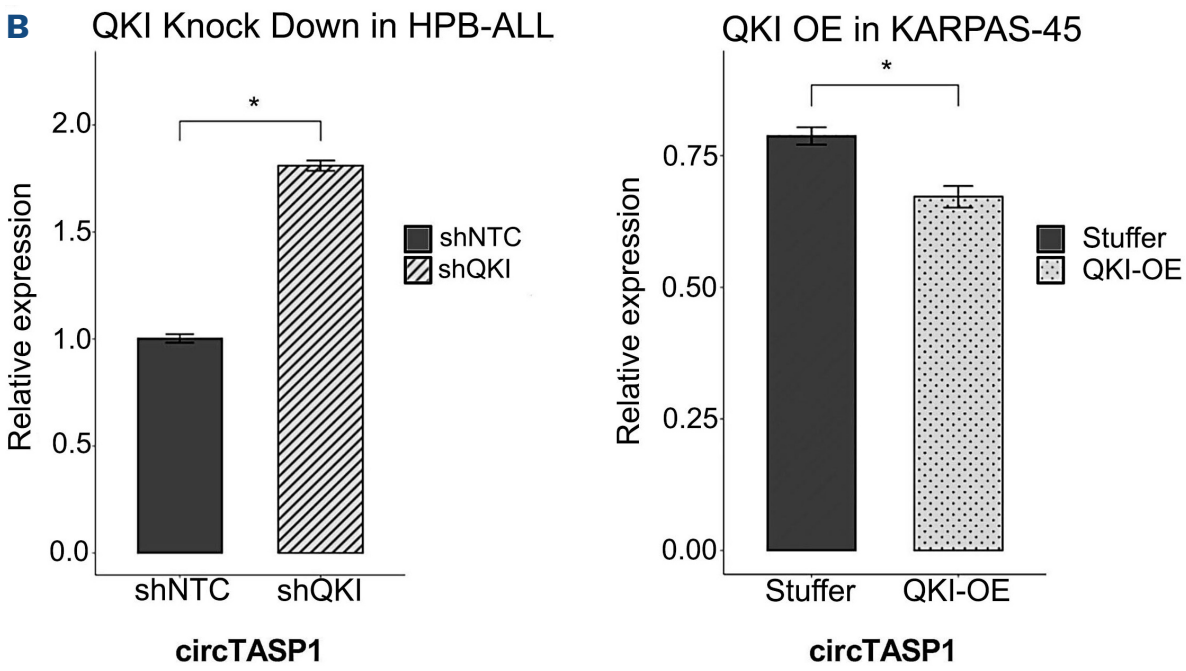

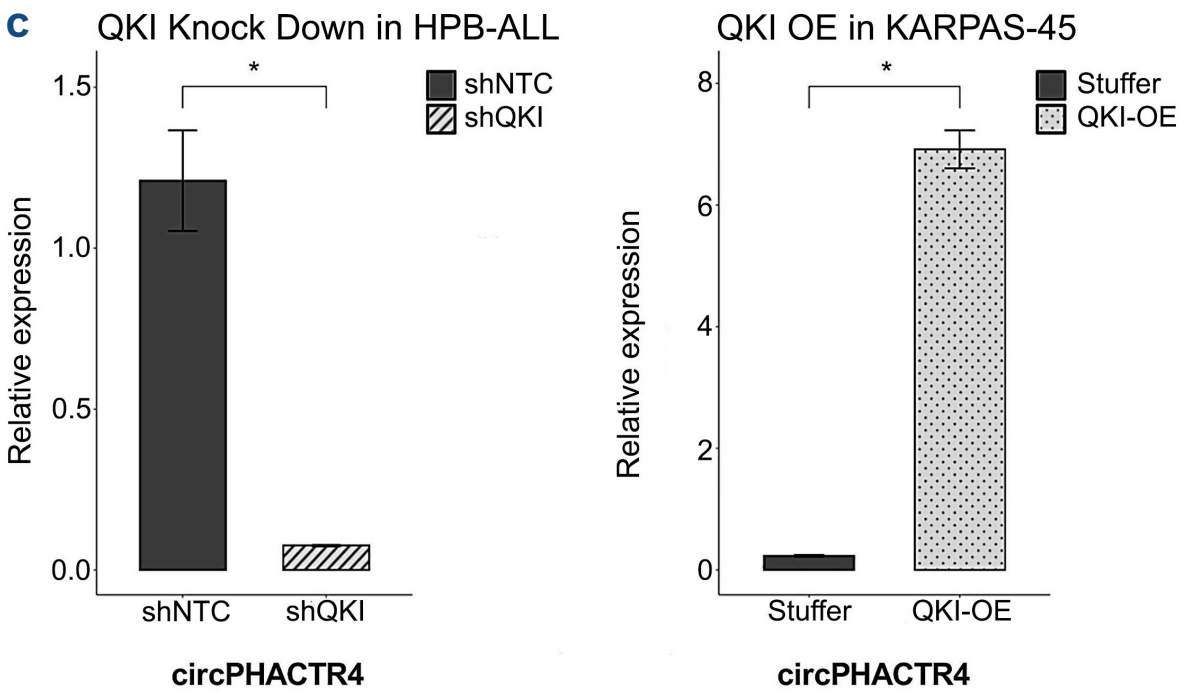

Figure 3. Circular RNA dependent on QKI expression in T-cell acute lymphoblastic leukemia. (A) Heatmap of 35 circular RNA (circRNA) with concordant expression change in the knockdown experiment (absolute log fold-change (LFC) >1 in QKI knockdown [KD] *vs.* control [CTR]) and significant absolute or relative (circular to linear, CLP) expression variation in QKI_low *versus* QKI_normal T-cell acute lymphoblastic leukemia (T-ALL); circRNA are clustered according to LFC values; the LFC in the comparison between QKI_low T-ALL and normal thymocytes and adjusted *P* value from the comparisons QKI_low *versus* QKI_normal T-ALL and QKI_low T-ALL *versus* thymocytes are also shown; estimated correlation with QKI expression level in T-ALL (rho); the discriminant property from the random forest model in T-ALL QKI-group classification (discriminant, YES or NO) and the average circRNA expression in T-ALL quantile (T-ALL Expr. Quantile, Q1-4). (B) CircTASP1 and (C) circPHACTR4 quantification by quantitative real-time polymerase chain reaction in HPB-ALL cells upon QKI KD and in Karpas-45 cells upon QKI overexpression (OE).

pared with normal thymocytes, were further investigated in Karpas-45 and HBP-ALL cell lines with respectively very low and high endogenous QKI expression. We obtained *QKI* silencing in HBP-ALL (85% reduction achieved). HEK293 cells were co-transfected with the envelope (pMD2.G), packaging (psPAX2) and shRNA TRC vector (MISSION®, Sigma-Aldrich) harboring a shRNA not targeting or targeting QKI (TRCN0000233373). HPB-ALL cells were transduced with viral particles (collected 72 hours and 96 hours after transfection and concentrated 10 times using PEG-it; System Biosciences) by spinoculation (2,300 rpm, 90 min, 32°C, 8 μg/mL polybrene H9268; Sigma-Aldrich). After 72 hours, 1 μg/mL of puromycin was included in the culture media for 7 days for the selection of transduced cells. We also obtained QKI overexpression in Karpas-45 cells (90 times increase achieved). HEK293 cells were co-transfected with the envelope, packaging and a lentiviral vector harboring an open reading frame (ORF) stuffer or the QKI ORF (pLV[Exp]-EF1A>ORF_Stuffer- CMV>Puro, VectorBuilder ID VB221221-1538ubv; pLV[Exp]-EF1A>hQKI[NM_006775.3]-CMV->Puro, VB221221-1535gjk). Viral production, transduction, selection and RNA extraction were performed as indicated above. Both experiments were performed four times. Real-time quantitative polymerase chain reaction analysis was used to quantify circTASP1 and circPHACT4 (circTASP1_F, GTAGGCTCCTTCTCCAACTA; circTASP1_R, CCCAGGCTGCTCTTTATG; circPHACTR4_F, GAAGGGCAAGCAAAGGAT; circPHACTR4_R, GCTTGAAGATCTTGCCAAAG; iScript™ cDNA Synthesis Kit; BioRad SsoAdvanced Universal SYBR® Green Supermix; Roche LightCycler® 480; CellCarta QBase+ software for data analysis).

A significant increase of circTASP1 was observed upon *QKI* silencing in HBP-ALL cells (Figure 3B), corroborating the dependency of this circRNA on QKI, with an indirect relation. CircTASP1 isoforms (exons 5-8, 4-7 and 8-10) are upregulated in T-ALL[2] and sustain acute myeloid leukemia

(exons 4-6).[15]

CircPHACTR4 was markedly decreased upon *QKI* silencing also in HBP-ALL, as in Jurkat cells and increased upon QKI overexpression in Karpas-45 cells (Figure 3B). Robust evidence was gathered of direct dependency of circPHACTR4 expression on the QKI level, concordantly in patients and in different T-ALL cell lines *in vitro*. The absolute decrease of circPHACTR4 was uncoupled from the variation of the linear counterpart and is likely due to a post-transcriptional modulation. This isoform is derived from the tumor suppressor gene *PHACTR4* which also produces a tumor suppressor circRNA (circPHACTR4 chr1:28473553-28476291; exons 6-7).[16] In the literature, QKI has been described to favor circRNA biogenesis, whereas we showed that a reduction in QKI can affect different circRNA groups in opposite ways, and provided experimental validation that QKI favors the expression of circPHACTR4 while suppressing circTASP1, suggesting a more complex picture.

In conclusion, T-ALL patients can be stratified by QKI expression and those with low QKI levels have a distinct circRNAome. In accordance with observations in patients, *QKI* silencing in T-ALL *in vitro* identified numerous circRNA with QKI-dependent absolute and relative expression. We unveiled reduced QKI expression as a novel factor that could explain, at least in part, circRNA dysregulation in T-ALL.

Authors

Alessia Buratin,[1] Bruno Palhais,[2-4] Enrico Gaffo,[1] Juliette Roels,[4] Julie Morscio,[4] Jolien Van Laere,[4] Silvia Orsi,[1,5] Geertruij te Kronnie,[1] Pieter Van Vlierberghe,[4] Panagiotis Ntziachristos[2-4] and Stefania Bortoluzzi[1]

[1]Department of Molecular Medicine, University of Padova, Padova, Italy; [2]Leukemia Therapy Resistance Unit, Department of Biomolecular Medicine, Ghent University, Ghent, Belgium; [3]Center for Medical Genetics, Ghent University and University Hospital, Ghent, Belgium; [4]Cancer Research Institute Ghent (CRIG), Ghent, Belgium and [5]Department of Biology, University of Padova, Padova, Italy

Correspondence:
S. BORTOLUZZI - stefania.bortoluzzi@unipd.it
https://doi.org/10.3324/haematol.2024.285971

Received: May 30, 2024.
Accepted: November 25, 2024.
Early view: December 5, 2024.

Disclosures

No conflicts of interest to disclose.

Contributions

AB, GtK, PVV and SB conceived the study. AB and SB were responsible for data selection, bioinformatic analysis and interpretation of the results. EG provided software. BP, EG, JR and SO collaborated on the bioinformatic analyses. BP, JM and JVL performed experiments. PN and SB supervised the project. AB, BP and SB wrote the manuscript. EG, GtK and PN revised the manuscript and all authors approved it.

Funding

SB is supported by Fondazione AIRC per la Ricerca sul Cancro (IG 2017 #20052 and IG#2023 #28966), EU funding within the MUR PNRR “National Center for Gene Therapy and Drugs based on RNA Technology” (Project N. CN00000041 CN3 Spoke #6 “RNA chemistry”) and “National Center for HPC, Big Data and Quantum Computing” (Project N. CN00000013 CN1 Spoke #8 “In Silico Medicine & Omics Data”), PRIN MIUR 2017 #2017PPS2X4_003 and PRIN MIUR 2022 #20222EC7LA. PN is supported by the Research Foundation Flanders (FWO, G0F4721N and G0A8B24N), start-up funds from the Department of Biomolecular Medicine, Ghent University, a Flanders interuniversity consortium grant (BOF. IBO.2023.0006.02) and a Cancer Research Institute Ghent (CRIG) partnership grant.

Data-sharing statement

RNA-sequencing data (GSE110636 and GSE142179) are freely available at Gene Expression Omnibus (*https://www.ncbi.nlm.nih.gov/geo/*).

References

1. Li Q, Ren X, Wang Y, Xin X. CircRNA: a rising star in leukemia. PeerJ. 2023;11:e15577.
2. Buratin A, Paganin M, Gaffo E, et al. Large-scale circular RNA deregulation in T-ALL: unlocking unique ectopic expression of molecular subtypes. Blood Adv. 2020;4(23):5902-5914.
3. Conn SJ, Pillman KA, Toubia J, et al. The RNA binding protein quaking regulates formation of circRNAs. Cell. 2015;160(6):1125-1134.
4. Gaffo E, Bonizzato A, Kronnie GT, Bortoluzzi S. CirComPara: a multi-method comparative bioinformatics pipeline to detect and study circRNAs from RNA-seq data. Noncoding RNA. 2017;3(1):8.
5. Chénard CA, Richard S. New implications for the QUAKING RNA binding protein in human disease. J Neurosci Res. 2008;86(2):233-242.
6. Bian Y, Wang L, Lu H, et al. Downregulation of tumor suppressor QKI in gastric cancer and its implication in cancer prognosis. Biochem Biophys Res Commun. 2012;422(1):187-193.

7. Bonizzato A, Gaffo E, Te Kronnie G, Bortoluzzi S. CircRNAs in hematopoiesis and hematological malignancies. Blood Cancer J. 2016;6(10):e483.
8. Tili E, Chiabai M, Palmieri D, et al. Quaking and miR-155 interactions in inflammation and leukemogenesis. Oncotarget. 2015;6(28):24599-24610.
9. Dik WA, Brahim W, Braun C, et al. CALM-AF10+ T-ALL expression profiles are characterized by overexpression of HOXA and BMI1 oncogenes. Leukemia. 2005;19(11):1948-1957.
10. Ferrando AA, Armstrong SA, Neuberg DS, et al. Gene expression signatures in MLL-rearranged T-lineage and B-precursor acute leukemias: dominance of HOX dysregulation. Blood. 2003;102(1):262-268.
11. Verboom K, Van Loocke W, Volders P-J, et al. A comprehensive inventory of TLX1 controlled long non-coding RNAs in T-cell acute lymphoblastic leukemia through polyA+ and total RNA sequencing. Haematologica. 2018;103(12):e585-e589.
12. Gaffo E, Buratin A, Dal Molin A, Bortoluzzi S. Sensitive, reliable and robust circRNA detection from RNA-seq with CirComPara2. Brief Bioinform. 2022;23(1):bbab418.
13. Wong CH, Lou UK, Fung FK-C, et al. CircRTN4 promotes pancreatic cancer progression through a novel CircRNA-miRNA-lncRNA pathway and stabilizing epithelial-mesenchymal transition protein. Mol Cancer. 2022;21(1):10.
14. Fu Z, Zhang P, Zhang R, et al. Novel hypoxia-induced HIF1α-circTDRD3-positive feedback loop promotes the growth and metastasis of colorectal cancer. Oncogene. 2023;42(3):238-252.
15. Lin Y, Huang Y, Liang C, Xie S, Xie A. Silencing of circTASP1 inhibits proliferation and induces apoptosis of acute myeloid leukaemia cells through modulating miR-515-5p/HMGA2 axis. J Cell Mol Med. 2021;25(15):7367-7380.
16. Wang Y, Yang Z, Gu J, et al. Estrogen receptor beta increases clear cell renal cell carcinoma stem cell phenotype via altering the circPHACTR4/miR-34b-5p/c-Myc signaling. FASEB J. 2022;36(2):e22163.